Andrographolide inhibits non-small cell lung cancer cell proliferation through the activation of the mitochondrial apoptosis pathway and by reprogramming host glucose metabolism

Zhao Chen^, Wei-Jian Tang, Yu-Han Zhou, Zhou-Miao Chen, Kai Liu

Department of Thoracic Surgery, Sir Run Run Shaw Hospital, School of Medicine, Zhejiang University, Hangzhou, China

Contributions: (I) Conception and design: K Liu; (II) Administrative support: K Liu; (III) Provision of study materials or patients: Z Chen; (IV) Collection and assembly of data: WJ Tang; (V) Data analysis and interpretation: YH Zhou; (VI) Manuscript writing: All authors; (VII) Final approval of manuscript: All authors.

Correspondence to: Kai Liu. Department of Thoracic Surgery, Sir Run Run Shaw Hospital, School of Medicine, Zhejiang University, No. 3, Qingchun Road East, Hangzhou 310016, China. Email: liukai720@zju.edu.cn.

Background: The main aim of this research was to explore the role and mechanism of Andrographolide (Andro) in controlling non-small cell lung cancer (NSCLC) cell proliferation.

Methods: Human NSCLC H1975 cells were treated with Andro (0–20 μM) for 4–72 h. B-cell leukemia/lymphoma 2 (Bcl-2)-antagonist/killer (Bak)-small interfering RNA (siRNA) (*Bak*-siRNA) and fructose-1,6-bisphosphatase (FBP1)-siRNA were transfected into H1975 cells to inhibit the endogenic Bak and FBP1 expression, respectively, and their expressions were detected by real-time quantitative reverse transcription–polymerase chain reaction (qRT-PCR) and western blotting (WB). Cellular proliferation ability was determined through various assessments, including 3-(4,5-dimethylthiazol-2-yl)-2,5-diphenyltetrazolium bromide (MTT), colony formation, and cell counting kit-8 (CCK-8) assays. Cell apoptosis ability was measured using flow cytometry. Pro-apoptotic-related proteins (*cleaved caspase 9*, *cleaved caspase 8*, and *cleaved caspase 3*) and mitochondrial apoptosis pathway proteins [Bcl2-associated X (*Bax*), *Bak*, *Bcl-2*, and cytochrome C (*cyto C*)] were assessed by WB. Aerobic glycolysis-associated genes [pyruvate kinase M2 (*PKM2*), lactate dehydrogenase A (*LDHA*), and glucose transporter 1 (*GLUT1*)] and gluconeogenesis genes [phosphoenolpyruvate carboxykinase 1 (*PEPCK1*), fructose-1,6-bisphosphatase 1 (*FBP1*), and phosphofructokinase (PFK)] were measured by qRT-PCR. The mitochondrial membrane depolarization sensor, 5, 50, 6, 60-tetrachloro-1, 10, 3, 30 tetraethyl benzimidazolo carbocyanine iodide (JC-1) assay was used for the measurement of mitochondrial membrane potential (ΔΨm). Additionally, glycolytic metabolism, lactate production, and adenosine triphosphate (ATP) synthesis were also analyzed.

Results: Andro inhibited human NSCLC cellular proliferation and induced apoptosis in a dose-time or dose-dependent manner via activation of the mitochondrial apoptosis pathway. Andro inhibited glycolysis, promoted the gluconeogenesis pathway, and increased the levels of *cleaved caspase 9*, *cleaved caspase 8*, *cleaved caspase 3*, *Bax*, *Bak*, *PEPCK1*, *FBP1*, and *PFK*, and decreased the levels of *Bcl-2*, *PKM2*, *LDHA*, and *GLUT1*. Moreover, it also decreased the ΔΨm and facilitated the release of cyto C from mitochondria into the cytoplasm. Furthermore, Andro enhanced the mitochondrial translocation of *Bak*, glucose uptake, lactate release, and intracellular ATP synthesis. Suppression of endogenic *Bak* and *FBP1* expression significantly reduced the effects of Andro in H1975 cells.

Conclusions: Andro represses NSCLC cell proliferation through the activation of the mitochondrial apoptosis pathway and by reprogramming glucose metabolism.

^ ORCID: 0000-0002-7623-4968.

Keywords: Non-small cell lung cancer (NSCLC); Andrographolide (Andro); cell proliferation; mitochondrial apoptosis pathway; glucose metabolism reprogramming

Submitted Oct 13, 2021. Accepted for publication Nov 23, 2021.
doi: 10.21037/atm-21-5975
View this article at: https://dx.doi.org/10.21037/atm-21-5975

Introduction

Despite modern epidemiological data and preventive therapies for lung cancer over the past decade, this disease is still the key cause of cancer deaths worldwide (1). In China, lung cancer morbidity and mortality remain the highest relative to other malignancies, which is consistent with global epidemiological data (2). Non-small cell lung cancer (NSCLC), a principal subtype of lung cancer, accounts for approximately 84% of new diagnoses (3). Although a variety of modern surgical treatments, targeted therapy, immunotherapy, and other treatment strategies have made breakthroughs in NSCLC, the 5-year survival rate remains relatively unchanged (11.15%). Additionally, the recurrence and mortality rates are still high (4,5). Therefore, further study of the pathogenesis of NSCLC and exploration of more effective treatment strategies are urgently required to improve disease outcomes.

Andrographolide (Andro) is a diterpenoid extracted from *Andrographis paniculata* (a traditional Chinese medicine). Andro is commonly used as an anti-inflammatory and detoxifying drug for the treatment of various infectious diseases (6). Recently, studies have found that in addition to its antiviral effects, Andro has potential anti-tumor activity (7,8). In an early review, it was hypothesized that Andro exerts anti-tumor activity in gastric, liver, lung, and breast cancers by boosting apoptosis, inducing cell cycle stagnation, and enhancing the anti-tumor activity of lymphocytes (9). Moreover, Andro was suggested as a possible anti-angiogenesis agent for human NSCLC, which acts by down-regulating vascular endothelial growth factor (*VEGF*), hypoxia-inducible factor-1α (*HIF-1α*), and transforming growth factor β1 (*TGF-β1*) to inhibit cell proliferation, tumor growth, angiogenesis, and lymph node metastasis (7,10). Andro also can be used as a potential ancillary drug. For example, it can enhance cisplatin-mediated anti-cancer effects by blockading autophagy and accelerating cisplatin-mediated apoptosis in lung cancer cells (11). In *in vitro* experiments, Andro was found to inhibit the migration and invasion of human NSCLC A549 cells via down-regulation of the phosphoinositide 3-kinase (*PI3K*)/protein kinase B (*Akt*) signaling pathway (12). Together, these lines of evidence suggest that Andro may be useful for the treatment of NSCLC; however, the inhibitory mechanism of NSCLC cell proliferation remains unclear.

Abnormal clonal proliferation of cells and uncontrolled apoptosis is the cause of tumor genesis and development. In general, cellular proliferation and apoptosis determine the fate of tumor cells. Additionally, investigations have illustrated that mitochondria perform an essential regulatory task during apoptosis and that mitochondrial dysfunction can lead to senescence and apoptosis in mammalian cells; both of which are related to the occurrence of various forms of cancer (13-17). Previous explorations have elucidated that the mitochondria-dependent apoptotic pathway is involved in apoptotic cell death of human NSCLC (18). Furthermore, the activation of the intrinsic mitochondrial apoptotic pathway can repress tumor proliferation and growth in NSCLC (19,20). So far, only one report has provided evidence to show that Andro has anti-cancer activity in human cancer cells by launching mitochondrial apoptosis pathway. For example, in lung carcinoma, Andro is able to induce cell death with the aid of the stimulation of the reactive oxygen species (ROS)-dependent mitochondrial apoptotic pathway (21). Together, these outcomes indicate that Andro may repress NSCLC cell proliferation via its effect on the mitochondrial apoptotic pathway.

Cancer cells are different from normal tissue cells. To meet the metabolic needs of the rapid proliferation of tumor cells, even if oxygen is sufficient, a large amount of glucose is needed for glycolysis to rapidly-produce enough substrate for synthesis and metabolism. Significantly enhanced aerobic glycolysis is an important feature of tumor glucose metabolism and is well-established as the "Warburg effect" (22). Tumor cells employ glycolytic metabolic pathways, which consume large amounts of glucose to produce high-energy metabolites (e.g., lactic acid, pyruvate) that are ingested by adjacent tumor cells and undergo mitochondrial oxidative phosphorylation (OXPHOS), thereby increasing tumor intracellular adenosine triphosphate

(ATP) production and promoting tumor cell proliferation, survival, growth, angiogenesis, invasion, and metastasis (23,24). The reverse reaction of glycolysis is gluconeogenesis. Metabolic enzymes of each process compete for substrate, resulting in antagonistic biochemical regulation (25). However, it remains unknown whether Andro inhibits NSCLC cell proliferation by reprogramming glucose metabolism. In the present research, we aimed to explore the performance of Andro in the inhibition of NSCLC cell proliferation through its activity on the mitochondrial apoptosis pathway and reprogramming glucose metabolism.

Based on the previous studies, the major innovations involved in this study were: (I) the treatment method on the basis of traditional Chinese medicine (Andro); (II) the molecular mechanism of Andro in treating NSCLC involving in mitochondrial apoptosis pathway-related genes; (III) the molecular mechanism of Andro in treating NSCLC involving in glucose metabolism pathway (glycolysis and gluconeogenesis-associated genes). We present the following article in accordance with the MDAR reporting checklist (available at https://dx.doi.org/10.21037/atm-21-5975).

Methods

Cell lines and cell culture

The human NSCLC (lung adenocarcinoma) cell line, H1975, was purchased from the American Type Culture Collection (ATCC) (Manassas, VA, USA). The cells were cultivated and maintained as previously described (26,27).

Cells transfection

For the knock-down of B-cell leukemia/lymphoma 2 (*Bcl-2*) -antagonist/killer (*Bak*) or fructose-1,6-bisphosphatase (*FBP1*) expression in H1975 cells, negative control (NC) (non-silencing control)-small interfering RNA (si-RNA) (NC-siRNA) and Bak targeting siRNA (*Bak*-siRNA) (50 nM) were acquired from Qiagen and transfected into the above target cells using the RNAiMAX transfection reagent (Invitrogen) according to the manufacturer's guidelines. NC-siRNA and *FBP1*-targeting siRNA (*FBP1*-siRNA) was designed and manufactured by Sangon Biotech Co., Ltd. (Shanghai, China), and the transfection was performed according to the lipofectamine 2000 kit (12,566,014, Thermo Fisher Scientific, Waltham, MA, USA) instructions. The transfection efficiency was ascertained through real-time quantitative reverse transcription–polymerase chain reaction (qRT-PCR) and western blotting (WB). After 48h of transfection with the si-RNAs, the cells were harvested for subsequent experiments.

Andro treatment

Andro was provided by Sigma-Aldrich (St Louis, Missouri, USA). It was then dissolved in dimethyl sulfoxide (DMSO) at varying concentrations (0, 2.5, 5, 10, 20 μM) based on the previously published literature (10,28). The Andro stocks were stored in a dark environment at –20 ℃. The varying concentrations of Andro mentioned above were added to cells for 0, 4, 8, 12, 16, 24, 48, and 72 h for following experiments, respectively.

3-(4,5-dimethylthiazol-2-yl)-2,5-diphenyltetrazolium bromide (MTT) assay

The influence of Andro on NSCLC cell growth was assessed using the MTT assay. Briefly, 5×10^4 cells/well of H1975 cells at the logarithmic growth phase were harvested and seeded into 96-well tissue culture plates. After the cells were adherent, Andro was added at diverse concentrations (0, 2.5, 5, 10, 20 μM), after which the cells were cultivated for 24, 48, and 72 h. The MTT solution was then added to the cells, which were cultured for an additional 4 h at 37 ℃. The culture milieu was discarded and 200 μL DMSO was added. Next, the plates underwent lucifugal oscillation for 15 min. The absorbance value (A value) at 490 nm of each well was determined by employing an automatic microplate reader (MK3, Thermo). The rate of cell survival was measured as previously described (29). The experiment was performed in triplicate.

Colony-formation assay

The clonal formation assay was implemented to measure the influence of Andro on NSCLC cell proliferation. Andro was added to H1975 cells at 0, 2.5, 5, 10, 20 μM. The cells were subsequently cultivated for 12 h. Thereafter, the cells were harvested and cultured in six-well tissue culture plates at a density of 5×10^3 cells/well for 2 weeks. After this period, the supernatant was eliminated, and the cells were fixed with 1 mL of 4% paraformaldehyde for 15 min followed by 1% crystal violet staining for 20 min. The colonies were counted under bright field microscopy and the cells' proliferative abilities were assessed. The experiment was repeated in triplicate.

Flow cytometry assays

Flow cytometry was implemented to assess the effect of Andro (0, 5, 10, 20 μM) on NSCLC cell apoptosis. After 24 h of Andro exposure, the cells were collected and stained with Annexin V-fluorescein isothiocyanate (FITC) (Beijing Biosea Biotechnology Co., Ltd., Beijing, China) and propidium iodide (PI), and then incubated at ambient temperature for 15 min in the dark. The cell apoptosis rate was scrutinized with the FACS Aria II (BD Biosciences) according to the manufacturer's instructions.

WB

The protein expressions of *cleaved caspase 9*, *cleaved caspase 8*, and *cleaved caspase 3* in H1975 cells, which were treated by diverse concentrations (0, 5, 10, 20 μM) of Andro for 24 h, were assessed through WB. H1975 cells processed with various concentrations (0, 20 μM) of Andro for 4, 8, 16 h, cytochrome C (*cyto C*), *Bak* (in mitochondria and cytoplasm), and *Bcl2*-associated X (*Bax*) were also assessed via WB.

NC-siRNA or *Bak*-siRNA transfected H1975 cells were processed with different concentrations (0, 5, 10, 20 μM) of Andro for 24 h, *Bcl-2*, *Bak*, *cleaved caspase 9*, *cleaved caspase 8*, and *cleaved caspase 3*. In NC-siRNA- or *FBP1*-siRNA-transfected H1975 cells, *FBP1*, *cleaved caspase 9*, *cleaved caspase 8*, and *cleaved caspase 3* were detected by WB. The isolation of mitochondrial and cytoplasmic proteins was achieved as previously shown (30). All WB experiments were conducted as previously published (31). The primary antibodies employed in this research were anti-human prohibitin as well as antibodies against the following: *FBP1* (ab109732) (1:1,000, Abcam, Shanghai, China); glyceraldehyde-3-phosphate dehydrogenase (*GAPDH*) (ab8245) (1:5,000, Abcam, Shanghai, China); *cyto C* (1:5,000, Abcam, Cambridge, MA, USA); *Bax* (1:400, Abcam, Cambridge, MA, USA); *Bak* (1:400, Abcam, Cambridge, MA, USA); *Bcl-2* (1:400, Abcam, Cambridge, MA, USA); *COX IV* (1:1,000, Cell Signaling Technology, Beverly, MA, USA); *cleaved caspase-3* (1:1,000, Cell Signaling Technology, Beverly, MA, USA); *cleaved caspase-8* (1:1,000, Cell Signaling Technology, Beverly, MA, USA); and *cleaved caspase-9* (1:1,000, Cell Signaling Technology, Beverly, MA, USA). The secondary antibodies were horseradish peroxidase (HRP)-conjugated goat anti-rabbit immunoglobulin G (*IgG*) (1:5,000, Abcam, Shanghai, China). *COX IV* was implemented as the internal reference for the mitochondrial protein, and *GAPDH* was employed as an internal reference for cytoplasmic protein assessment. All protein bands were quantified using the ImageJ computer program (National Institutes of Health, Bethesda, MD, USA).

Assessment of mitochondrial membrane potential (ΔΨm)

After different concentrations (0, 20 μM) of Andro acting on H1975 cells for 16 h, or after 20 μM of Andro acting on H1975 cells (transfected with NC-siRNA or Bak-siRNA) for 24 h, the cells were collected for ΔΨm analyses using the ΔΨm assay kit with cationic mitochondrial membrane depolarization sensor, 5, 50, 6, 60-tetrachloro-1, 10, 3, 30 tetraethyl benzimidazolo carbocyanine iodide (JC-1) (Beyotime; Shanghai, China) fluorescence staining, according to manufacturer's instructions. The operational details were cited as previously described (32).

qRT-PCR

The messenger RNA (mRNA) expressions of *Bak* in H1975 cells transfected with NC-siRNA or *Bak*-siRNA, *FBP1* in H1975 cells transfected with NC-siRNA or *FBP1*-siRNA, the aerobic glycolysis-related genes [pyruvate kinase M2 (*PKM2*)], lactate dehydrogenase A (*LDHA*), glucose transporter 1 (*GLUT1*), gluconeogenesis-related genes [phosphoenolpyruvate carboxykinase 1 (*PEPCK1*)], fructose-1,6-bisphosphatase 1 (*FBP1*), and phosphofructokinase (*PFK*) in H1975 cells, which were processed with Andro (0, 20 μM) for 24 h, were detected by qRT-PCR.

Total RNA was extracted using the RNeasy kit (Qiagen, Valencia, CA) according to the manufacturer's protocol, and quantified using the Nanodrop 2000 spectrophotometer (Thermo Fisher Scientific, Inc.). Complementary DNA (*cDNA*) was synthesized using a reverse transcription kit (Applied Biosystems, Foster City, CA, USA). The PCR primers employed in the present survey were designed and prepared by Beijing ComWin Biotech Co. Ltd. (Beijing, China) and are listed in *Table 1*. For data normalization, *β-actin* was employed as the internal reference. PCR reactions were performed on an ABI 7500 Real-Time PCR system (Applied Biosystems), the relative expressions were quantified using the $2^{-\Delta\Delta Ct}$ approach.

Cell Counting Kit-8 (CCK-8) assay

After 24 h of 20 μM Andro exposure, the cellular proliferation of H1975 cells (transfected with NC-siRNA/

Table 1 Gene primer sequences

Gene	Forward primer	Reverse primer
Bak	5'-TGAGTACTTCACCAAGATTCA-3'	5'-AGTCAGGCCATGCTGGTAGAC-3'
FBP1	5'-GGTGGACAAGGATGTGAAGATA-3'	5'-GGGAACTTCTTCCTCTGGATG-3'
PKM2	5'-CTTGCAATTATTTGAGGAACTCCGC-3'	5'-CACGGTACAGGTGGGCCTGAC-3'
LDHA	5'-AAGCGGTTGCAATCTGGATTCAG-3'	5'-GGTGAACTCCCAGCCTTTCC-3'
GLUT1	5'-GATTGGCTCCTTCTCTGTGG-3'	5'-TCAAAGGACTTGCCCAGTTT-3'
PEPCK1	5'-GCTCTGAGGAGGAGAATGG-3'	5'-TGCTCTTGGGTGACGATAAC-3'
PFK	5'-GGTGGACGGAGGAGATAACA-3'	5'-CAGTCAGGGAACCATCACCT-3'
β-actin	5'-CAGCCTTCCTTCCTGGGCATG-3'	5'-ATTGTGCTGGGTGCCAGGGCAG-3'

Bak, Bcl-2-antagonist/killer (Bak); *FBP1*, fructose-1,6-bisphosphatase 1; *PKM2*, pyruvate kinase M2; *LDHA*, lactate dehydrogenase A; *GLUT1*, glucose transporter 1; *PEPCK1*, phosphoenolpyruvate carboxykinase 1; *PFK*, phosphofructokinase.

Bak-siRNA or NC-siRNA/FBP1-siRNA) was assessed using the CCK-8 assay kit (Boster, Wuhan, China) as previously described (33). After the addition of the CCK-8 solution, absorbance values at 450 nm were recorded at 24, 48, and 72 h, accordingly. The assay was conducted in triplicate.

Measurement of glucose uptake, lactate release, and intracellular ATP synthesis

After different concentrations (0, 20 μM) of Andro acting on H1975 cells for 24 h, or after 20 μM of Andro acting on H1975 cells (transfected with NC-siRNA or *FBP1*-siRNA) for 24 h, the cells were gathered for preparations of cell lysis buffer. The levels of lactate production and glucose uptake were determined according to the instructions of the glucose uptake colorimetric assay kit (BioVision, Milpitas, CA, USA) and lactate assay kit (BioVision, Milpitas, CA, USA), respectively. The operating steps were described as previously reported (26). The intracellular ATP level was quantitatively determined by employing the CellTiter-Glo Luminescent Cell Viability Assay kit (Promega, Madison, WI) according to the manufacturer's protocol, and the specific procedures were referenced to the previously published report (34).

Statistical analysis

Statistical Package for the Social Sciences (SPSS) version 21.0 was employed for the statistical analysis of all data. The obtained outcomes are shown as means ± standard deviation (SD) and percentage/rate (%). Quantitative data between the two groups were scrutinized using the independent-samples *t*-test and the Student's *t*-test. Percentage/rate data between groups were assessed with the χ^2 test or non-parametric Mann-Whitney U test or Fisher's exact test. All continuous data were tested for normality using the Anderson-Darling method. The statistical significance level was set as P values <0.05.

Results

Andro inhibits NSCLC cell proliferation

To evaluate the function of Andro on NSCLC cell proliferation, the MTT assay was performed to determine the cell survival rate of H1975 cells. Andro treatment with disparate concentrations of 0, 2.5, 5, 10, and 20 μM for 24, 48, and 72 h were utilized. Colony enumeration was used to determine the clonogenic formation potential of H1975 cells treated by a range of concentrations (0, 2.5, 5, 10, 20 μM) of Andro for 12 h. After Andro treatment, the cell survival rate and the clonal formation rate/percentage were significantly reduced in a concentration/dose-time dependent manner compared to the unprocessed controls (P<0.05, P<0.01, P<0.001, respectively) (*Figure 1A*,*1B*).

Andro promotes NSCLC cell apoptosis

After the H1975 cells were processed with diverse concentrations (0, 5, 10, 20 μM) of Andro for 24 h, cell apoptosis was estimated by flow cytometry and WB (*Figure 2A*,*2B*). Compared to the unprocessed controls, Andro treatment markedly boosted H1975 cell apoptosis,

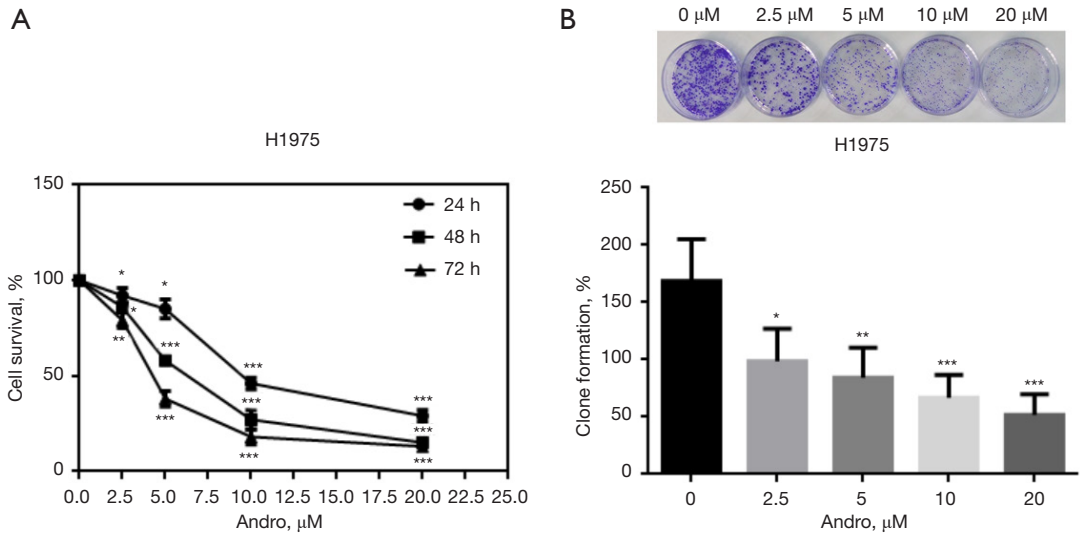

Figure 1 Andro suppresses NSCLC cell proliferation. (A) Andro inhibited H1975 cell survival in a dose-time-dependent manner, as measured by MTT assessment; (B) Andro inhibited H1975 cell clone formation in a dose-dependent manner, as measured through the colony-formation assay. Colony formation capacities were determined by crystal violet staining and the magnification was 40× under optical microscope. *, P<0.05; **, P<0.01; ***, P<0.001. Andro, andrographolide; NSCLC, non-small cell lung cancer; MTT, 3-(4,5-dimethylthiazol-2-yl)-2,5-diphenyltetrazolium bromide.

with an increased apoptotic cell rate and increased proteins levels of *cleaved caspase 9*, *cleaved caspase 8*, and *cleaved caspase 3* in a dose-dependent manner (P<0.05, P<0.01, P<0.001).

Andro inhibits NSCLC cell proliferation by activating the mitochondrial apoptosis pathway

To determine whether Andro exerted anti-cancer effects through the activation of the mitochondrial apoptosis pathway in NSCLC, mitochondrial membrane potential (ΔΨm), *cyto C* release, *Bak* mitochondrial translocation, and mitochondrial apoptosis pathway-associated proteins (*Bax*, *Bak*, *Bcl-2*) were analyzed. JC-1 fluorescence was used to measure the ΔΨm of H1975 cells that were processed with Andro (0 and 20 μM) for 16 h. In the Andro treatment group, a significant decline in ΔΨm with a decreased red/green fluorescence ratio at a wavelength of 488 nm was observed relative to the control cells (P<0.01) (*Figure 3A*). Moreover, the WB outcomes illustrated that compared to the control group, the protein expression level of mitochondrial *cyto C* was decreased and cytoplasmic *cyto C* was increased in H1975 cells after Andro treatment at 4 h (P<0.05), 8 h (P<0.01), and 16 h (P<0.001) (*Figure 3B*). These data indicated that *cyto C* was released from mitochondria into the cytoplasm during Andro treatment. In contrast, mitochondrial *Bak* protein expression was increased and cytoplasmic *Bak* was decreased in H1975 cells after Andro treatment at 4 h (P<0.05), 8 h (P<0.01), and 16 h (P<0.001). These data indicate that *Bak* mitochondrial translocation occurred (*Figure 3B*).

Meanwhile, after 24 h of Andro treatment (0, 5, 10, 20 μM), *Bax* and *Bak* protein expressions were dose-dependently up-regulated, while *Bcl-2* was down-regulated, relative to the control cells (*Figure 3C*) (P<0.05/P<0.01/P<0.001). To further validate this observation, the mRNA and protein levels of *Bak* were knocked-down using *Bak*-siRNA (*Figure 3D*) (P<0.01). At 48 h post-transfection, the H1975 cells were subjected to 20 μM of Andro for 24 h, after which cell proliferation ability, ΔΨm, and pro-apoptotic proteins were detected using the CCK-8 assay, JC-1 fluorescence staining, and WB, respectively. These findings demonstrated that compared to the NC-siRNA group, the *Bak*-siRNA group exhibited enhanced cell proliferation ability (*Figure 3E*) (P<0.05/P<0.01), increased the ΔΨm (*Figure 3F*) (P<0.001), and decreased the expressions of *cleaved caspase 9*, *cleaved caspase 8*, and *cleaved caspase 3* protein (*Figure 3G*) (P<0.001). These results suggested that *Bak* is a key molecule in the inhibition of NSCLC cell proliferation through the Andro-induced mitochondrial apoptosis pathway.

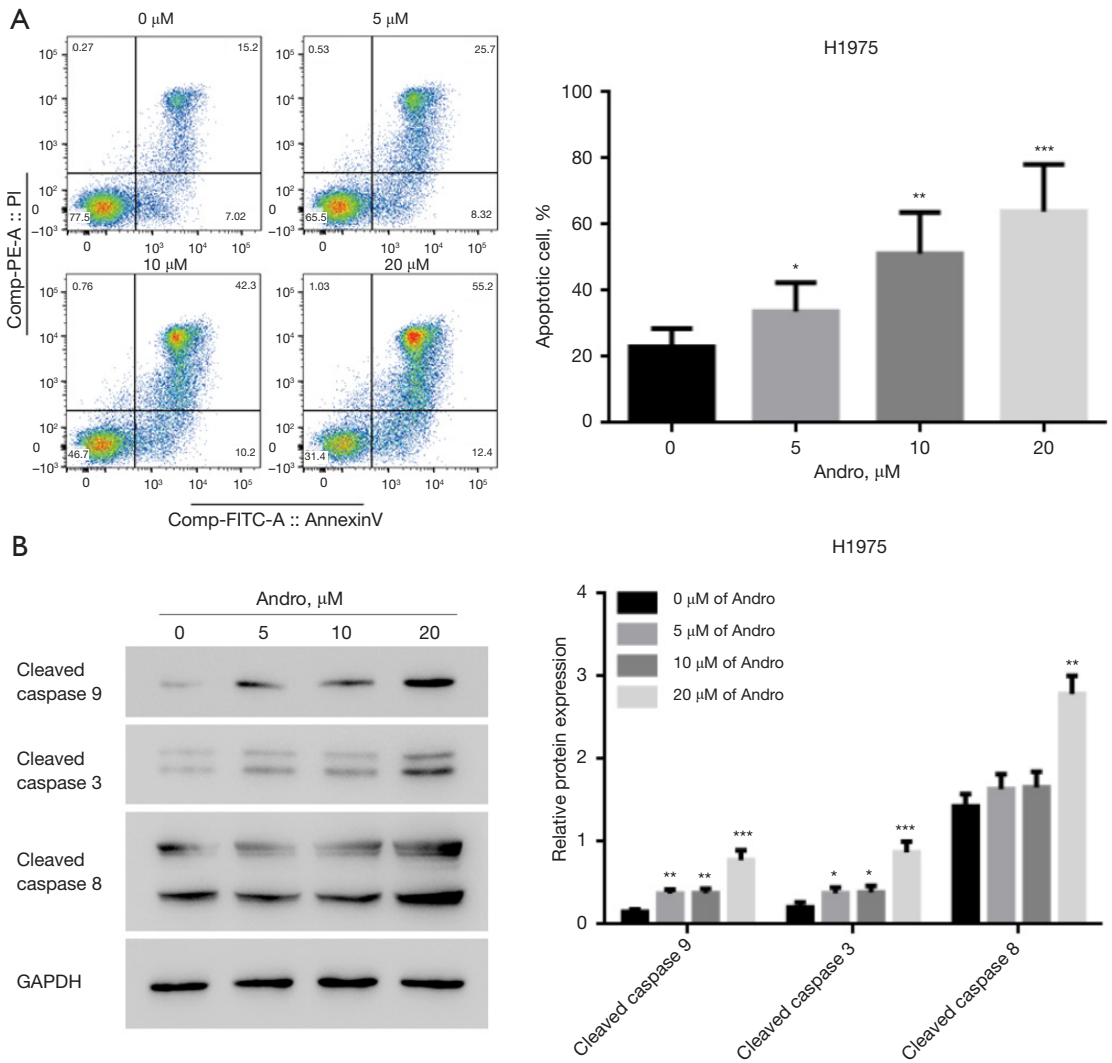

Figure 2 Andro exposure promotes NSCLC cell apoptosis. (A) Andro facilitated H1975 cell apoptosis in a dose-dependent manner, as measured through flow cytometry; (B) Andro enhanced *cleaved caspase 9*, *cleaved caspase 8*, and c*leaved caspase 3* expression in H1975 cells in a dose-dependent manner, as measured by WB. *, P<0.05; **, P<0.01; ***, P<0.001. Andro, andrographolide; NSCLC, non-small cell lung cancer; WB, western blotting.

Andro suppresses NSCLC cell proliferation by inducing glucose metabolism reprogramming

At 24 h post-Andro treatment (0, 20 μM), the mRNA level of aerobic glycolysis-related genes (*PKM2*, *LDHA*, and *GLUT1*) and the gluconeogenesis-related genes (*PEPCK1*, *FBP1*, and *PFK*) were measured with qRT-PCR. Additionally, lactate production, glucose uptake, and intracellular ATP level were also determined. The mRNA expressions of *PKM2*, *LDHA*, and *GLUT1* were decreased, while those of *PEPCK1*, *FBP1*, and *PFK* were significantly increased in the Andro treatment group relative to the control group (*Figure 4A*) (P<0.05/P<0.01). Moreover, Andro treatment markedly reduced the lactate production, glucose uptake, and intracellular ATP level (*Figure 4B*) (P<0.05/P<0.01).

For further validation, endogenous *FBP1* expression was successfully knocked down in H1975 cells via transfection with *FBP1*-siRNA (*Figure 4C*). At 48 h post siRNA transfection, the cells were processed with 20 μM of Andro for 24 h. Lactate production, glucose uptake, intracellular ATP level, cell proliferation ability, and pro-

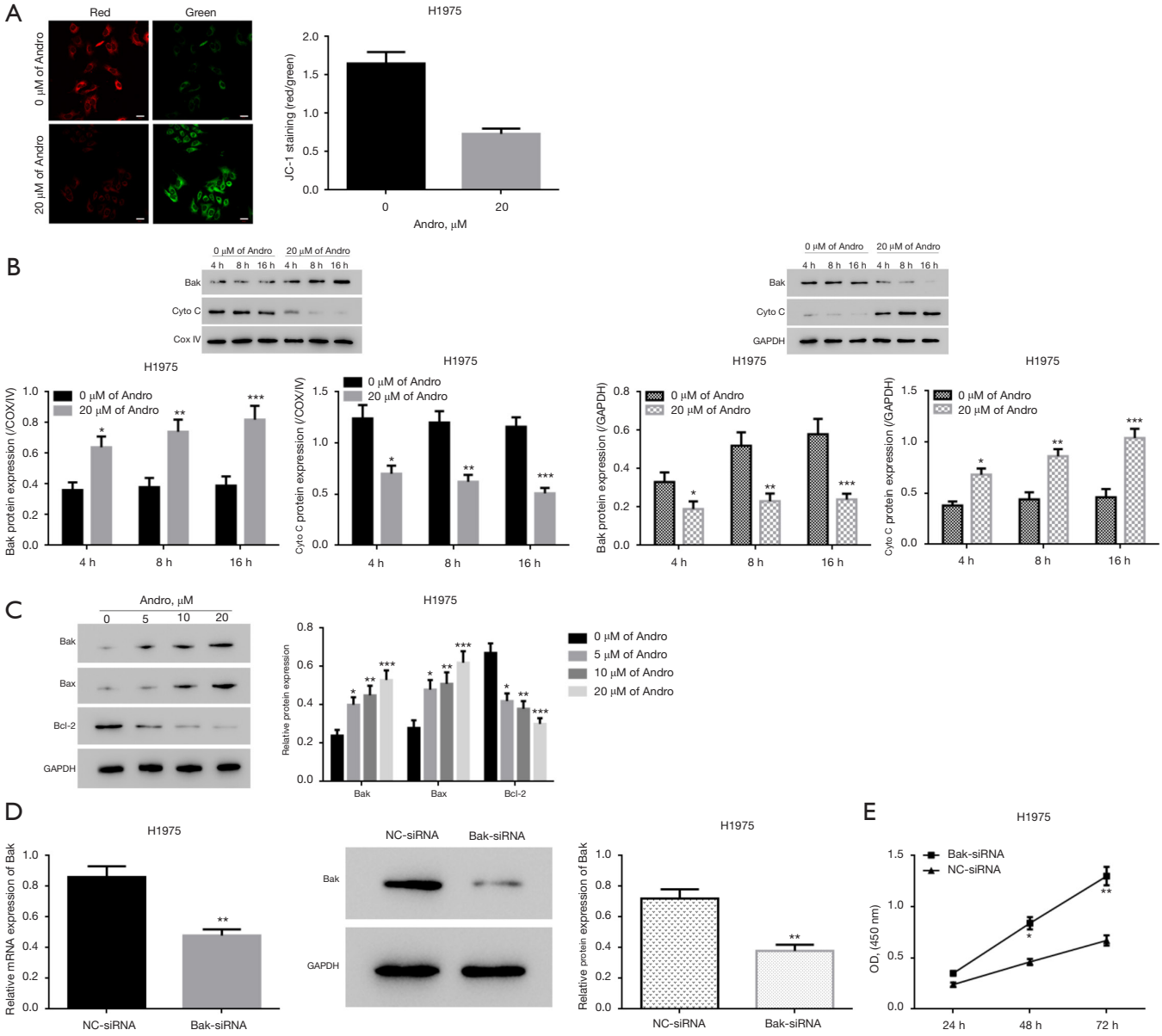

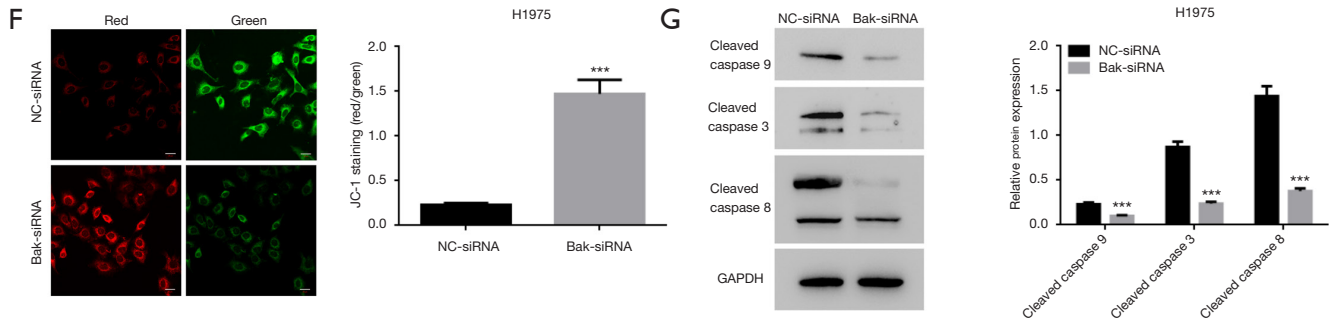

Figure 3 Andro inhibits NSCLC cell proliferation by activating the mitochondrial apoptosis pathway. (A) Andro weakened ΔΨm in H1975 cells, as measured by JC-1 fluorescence. Scale bar: 20 μm; (B) Andro inhibited mitochondrial cyto C and cytoplasmic Bak expressions, and promoted cytoplasmic cyto C and mitochondrial Bak expressions in H1975 cells in a time-dependent manner, as evaluated through WB; (C) Andro enhanced Bax and Bak and inhibited Bcl-2 expression in H1975 cells in a dose-dependent manner, as evaluated through WB; (D) Transfection with Bak-siRNA significantly inhibited Bak mRNA and protein expressions in H1975 cells, as determined by qRT-PCR and WB, respectively; (E) Bak downregulation promoted H1975 cell proliferation, as measured through CCK-8 assay; (F) Bak downregulation enhanced ΔΨm in H1975 cells, as determined by the JC-1 fluorescence experiment. Scale bar: 20 μm; (G) Bak downregulation markedly inhibited apoptotic executive proteins (cleaved caspase 9, cleaved caspase 8, and cleaved caspase 3) expression in H1975 cells, as measured by WB. *, P<0.05; **, P<0.01; ***, P<0.001. Andro, andrographolide; NSCLC, non-small cell lung cancer; ΔΨm, mitochondrial membrane potential; JC-1: mitochondrial membrane depolarization sensor, 5, 50, 6, 60-tetrachloro-1, 10, 3, 30 tetraethyl benzimidazolo carbocyanine iodide; cyto C, cytochrome C; Bcl-2, B-cell leukemia/lymphoma 2; Bak, Bcl-2-antagonist/killer (Bak); Bax, Bcl2-associated X; GAPDH, glyceraldehyde-3-phosphate dehydrogenase; Mrna, messenger RNA; WB, western blotting; qRT-PCR, real-time quantitative reverse transcription-polymerase chain reaction; CCK-8, cell counting kit-8; OD, optical density; NC, negative control; si, small interfering.

apoptotic proteins were assessed. Compared to the NC-siRNA control group, the *FBP1*-siRNA group showed increased lactate production, glucose uptake, intracellular ATP synthesis (*Figure 4D*) (P<0.05/P<0.01), enhanced cell proliferation ability (*Figure 4E*) (P<0.05/P<0.01), and reduced *cleaved caspase 9*, *cleaved caspase 8*, and *cleaved caspase 3* protein levels (*Figure 4F*) (P<0.01). Together, these data indicate that FBP1 is a key molecule in the remodeling of the Andro-induced glucose metabolism patterns, which can inhibit NSCLC cell proliferation.

Discussion

There is growing evidence to support the hypothesis that both the mitochondrial apoptosis pathway (35-37) and glucose metabolism reprogramming/"Warburg effect" (38,39) perform essential tasks in the advancement of certain types of cancer. For example, Apicidin can repress NSCLC GLC-82 cell proliferation and invasion as well as promote apoptosis by regulating the mitochondrial pathway (40). The knockdown of gasdermin-D (*GSDMD*) can attenuate tumor proliferation by promoting the intrinsic mitochondrial apoptotic pathway in NSCLC (18). Moreover, the inhibition of glucose metabolism is conducive to the suppression of NSCLC proliferation, colony formation, acceleration of cell-cycle arrest, and apoptosis (41).

Recently, several studies have shown that Andro, a traditional Chinese medicine, may exert anti-cancer activity through the suppression of cell proliferation, tumor growth, migration, invasion, angiogenesis, and lymph node metastasis in NSCLC (7,10,12). However, a comprehensive understanding of how Andro affects NSCLC cell proliferation and its role in the mitochondrial apoptosis pathway in NSCLC is lacking. Furthermore, it is also unknown if Andro affects the underlying molecular mechanisms related to glucose metabolism reprogramming in NSCLC. Herein, we showed that Andro inhibits NSCLC H1975 cell proliferation, colony formation, and advances cell apoptosis by activating the mitochondrial apoptosis pathway and mediating glucose metabolism reprogramming through the modulation of gene expression.

Initially, we found that Andro remarkably repressed human NSCLC H1975 cell proliferation, which was reflected by the repression of cell survival in a

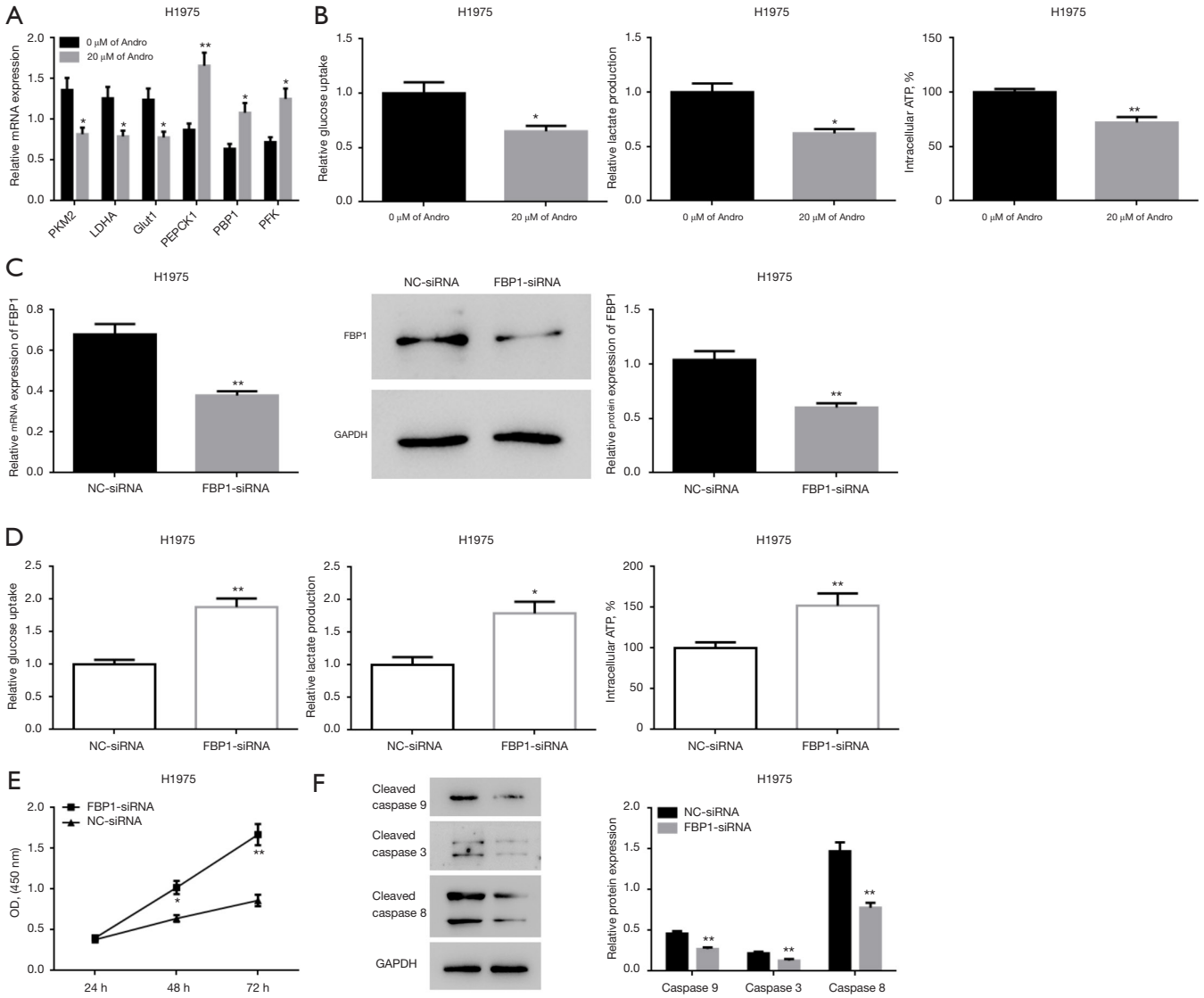

Figure 4 Andro suppresses NSCLC cell proliferation by inducing the reprogramming of glucose metabolism. (A) Andro reduced the expression of *PKM2*, *LDHA*, and *GLUT1* genes, and stimulated the expression of *PEPCK1*, *FBP1*, and *PFK* genes in H1975 cells, as measured by qRT-PCR; (B) Andro inhibited glucose uptake, lactate production, and intracellular ATP synthesis in H1975 cells; (C) *FBP1*-siRNA significantly inhibited *FBP1* expression at both the mRNA and protein levels in H1975 cells, as measured by qRT-PCR and WB; (D) in H1975 cells, FBP1 downregulation promoted glucose uptake, lactate production, intracellular ATP synthesis; (E) *FBP1* downregulation promoted H1975 cell proliferation, as evaluated through the CCK-8 assay; (F) FBP1 downregulation inhibited *cleaved caspase 9*, *cleaved caspase 8*, and *cleaved caspase 3* gene expression, as evaluated through WB. *, P<0.05; **, P<0.01. Andro, andrographolide; NSCLC, non-small cell lung cancer; *PKM2*, pyruvate kinase M2; *LDHA*, lactate dehydrogenase A; *GLUT1*, glucose transporter 1; *PEPCK1*, phosphoenolpyruvate carboxykinase 1; *FBP1*, fructose-1,6-bisphosphatase 1; *PFK*, phosphofructokinase; *GAPDH*, glyceraldehyde-3-phosphate dehydrogenase; ATP, adenosine triphosphate; qRT-PCR, real-time quantitative reverse transcription-polymerase chain reaction; Mrna, messenger RNA; WB, western blotting; CCK-8, cell counting kit-8; OD, optical density; NC, negative control; si, small interfering.

concentration/dose-time dependent manner. Additionally, our data showed that Andro inhibited clonal creation in a dose-dependent manner (*Figure 1*). Homoplastically, Andro induces cell apoptosis and increases the pro-apoptotic protein expression of *cleaved caspase 9*, *cleaved caspase 8*, and *cleaved caspase 3* in a dose-dependent manner in NSCLC (*Figure 2*). These findings are consistent with data reported by Luo *et al.* [2014], who showed that Andro could inhibit NSCLC H3255 cell proliferation in a dose-dependent manner (10). The authors concluded that Andro could restrain tumor growth and promote cell apoptosis in NSCLC (A549 and LLC) cells-seeded NSCLC mice (11). Additionally, Andro has been reported to inhibit NSCLC A549 cell proliferation in a dose-dependent manner, and induce the A549 cell-cycle arrest at the G2/M phase as well as apoptosis (42). The data reported here strongly support the findings of these studies.

Next, we found that Andro activated the mitochondrial apoptosis pathway in human NSCLC H1975 cells. This activation may stimulate cell apoptosis and inhibit cell proliferation. Here, Andro treatment was found to reduce ΔΨm (*Figure 3A*), induce *cyto C* mitochondrial release and *Bak* mitochondrial translocation (*Figure 3B*), enhance the expressions of pro-apoptotic proteins (*Bax* and *Bak*), and reduce the expression of the anti-apoptotic protein *Bcl-2* (which is the molecular marker of the mitochondrial apoptotic pathway) (*Figure 3C*). Moreover, we knocked down Bak expression in H1975 cells (*Figure 3D*) and assessed cellular sensitivity to an Andro-induced increase in pro-apoptotic proteins (*cleaved caspase 9*, *cleaved caspase 8*, and *cleaved caspase 3*) (*Figure 3G*) and inhibition of cell proliferation (*Figure 3E*). Furthermore, in knocked-down cells, ΔΨm (*Figure 3F*) was also significantly reduced.

The mitochondria apoptosis pathway is involved in drug-mediated cell death (19). Disruption of ΔΨm (one of the earliest intracellular events) usually occurs in apoptosis (43). The loss of ΔΨm is a substantial event in the mitochondrial apoptosis pathway (21). Previous reports have elucidated that Andro treatment in cancer cells facilitates a loss of ΔΨm (44). Moreover, Andro has been shown to affect drug-induced human lung cancer NCI-H292 cell death through the activation of the mitochondria-dependent pathway accompanied by a reduced ΔΨm (20). When ΔΨm decreases, *cyto C* binds to *caspase-9*, resulting in the activation of *caspase-3*, which results in apoptosis (45).

The *Bcl-2* protein family (including anti-apoptotic *Bcl-2* family proteins like *Bcl-2* and pro-apoptotic *Bcl-2* family proteins such as *Bax* and *Bak*) apoptotic and anti-apoptotic protein interactions play a critical role in the mitochondrial apoptosis pathway (19,44). *Bax* induces apoptosis by facilitating the formation of a channel into the outer mitochondrial membrane. This results in *Bak* mitochondrial translocation and the release of *cyto C* from mitochondria into the cytoplasm (19). Cytoplasmic *cyto C* is related to activated *caspase-9* and *caspase-3*, and can cause early apoptosis through the intrinsic mitochondrial pathway (19,46). Caspases promote cell apoptosis by fragmenting DNA. *Caspase-9* is activated during the early stage of the caspase-dependent mitochondrial apoptosis pathway. Following activation, *caspase-9* initiates the activation of *caspase-8*, which can directly activate *caspase-3* (21,47). Abnormal clonal proliferation, deregulatory apoptosis, and uncontrolled cell-cycle progression are the basic characteristics of cancer. Uncontrolled cellular apoptosis is the cause of abnormal clonal proliferation. Thus, based on these data as well as our current findings, it is clear that Andro inhibits NSCLC cell proliferation by inducing apoptosis via the activation of the mitochondrial pathway.

Furthermore, we found that Andro treatment down-regulated the expression of aerobic glycolysis-related genes (*PKM2*, *LDHA*, and *GLUT1*) and upregulated the expression of gluconeogenesis-related genes (*PEPCK1*, *FBP1*, and *PFK*) (*Figure 4A*). Andro treatment resulted in a diminution in glucose uptake, lactate production, and intracellular ATP levels (*Figure 4B*). Moreover, in H1975 cells with reduced endogenous *FBP1* expression (*Figure 4C*), Andro increased cell sensitivity to pro-apoptotic proteins (*cleaved caspase 9*, *cleaved caspase 8*, and *cleaved caspase 3*) (*Figure 4F*), repressed cell proliferation (*Figure 4E*), and increased lactate production and glucose uptake. Furthermore, the intracellular ATP level (*Figure 4D*) was significantly decreased. Previous work has identified an altered glucose metabolic program as one of the key hallmarks of cancer (48). In cancer cells, glycolysis predominantly occurs in the cytosol rather than in mitochondria. Intensive glycolysis/the "Warburg effect" is largely the result of canceration (49,50). In contrast, gluconeogenesis is mitigative in oncogenic lesions (51,52). Intensive gluconeogenesis acts as a tumor repressor that hinders aerobic glycolysis and the occurrence of the "Warburg effect" (53). To distinguish cancer cells from normal cells, an accelerated aerobic glycolysis has been found, and this high aerobic glycolysis level has been used as a hallmark for developing some diagnostic techniques for detecting image tumours *in vivo* (39). Inhibition of glycolysis can induce tumor cells apoptosis and facilitate cell proliferation

significantly *in vitro* and inhibit tumor growth in animal models (54,55). In clinical, 2-Deoxy-2-[18F] fluoroglucose (^{18}F-FDG) (a ^{18}F marked glucalogue) is widely used in tumor localization and mapping (56) and approved by the FDA for the diagnosis of suspected or existing cancers. In early and locally advanced NSCLC, ^{18}F-FDG PET/CT are recommended technique for clinical diagnosis and staging, respectively (57). You *et al.* (58) used isotope-labeled glucose (1, 2-$^{13}C_2$-glucose) combined with glucose uptake and lactate secretion to determine the relative activity of glycolysis and PPP pathways. It was demonstrated that in sorafenib-resistant cells, the glycolysis pathway was enhanced while the glucose flux through PPP was reduced. Hyperpolarized [1-^{13}C] pyruvate metabolism with 13C magnetic resonance spectroscopy imaging (MRSI) has been shown to be an early indicator of therapeutic response of tumor. *GLUT1*, a glucose transporter, can repress tumor growth by stimulating glucose uptake (59). Due to the "Warburg effect", glucose uptake is commonly enhanced in cancer to meet the high energy demand and compensate for the low ATP-generating efficiency (60). Lactate dehydrogenase A (*LDHA*), an enzyme involved in the final step of glycolysis that catalyzes pyruvate into lactate, was identified as a potential predictor of prognosis in NSCLC patients (61). In osimertinib-resistant NSCLC cells, glycolysis is augmented and a significantly upregulated glucose uptake and lactate production level has been observed (26).

In cancer cells, enhanced glycolysis is favorable for ATP generation and is associated with the promotion of cancer advancement and progression (62). In contrast, the inhibition of ATP production is conducive to triggering human lung cancer cell death (63). Interestingly, the essential function of mitochondria is to produce ATP, and thus, mitochondria could perform an essential secondary task in the "intrinsic" apoptosis pathway (64,65). Together, these lines of evidence imply that the mitochondrial apoptosis pathway and the reprogramming of glucose metabolism may synchronize in cancer progression. *PKM2* is a leading enzyme that regulates aerobic glycolysis in tumor cells; *PKM2*-mediated regulation can promote tumor growth and inhibit cancer cell apoptosis by enhancing ATP synthesis (66). *FBP1*, a rate-limiting enzyme in gluconeogenesis, plays a tumor-suppressive role by inducing glycolysis inhibition during lung cancer progression (67). *PEPCK1*, another rate-limiting enzyme in gluconeogenesis, suppresses tumor formation by increasing gluconeogenesis, suppressing glycolysis, and promoting ATP depletion and cell growth arrest (68). Increased gluconeogenesis is often ascribed to increased *PEPCK1* (cytosolic form) levels (69). *PFK*, a key glycolytic/rate-limiting enzyme in gluconeogenesis, catalyzes the first irreversible reaction of glycolysis to promote glucose consumption (70), and thus, may further accelerate apoptosis (71). Our data are consistent with previously reported findings showing that Andro suppresses NSCLC cell proliferation by inducing glucose metabolism reprogramming.

For research value or significance, it is listed as follows: (I) we elaborated the anti-cancer effect and mechanism of Andro in treating NSCLC, which have enriched scientific evidences for traditional Chinese medical (TCM) therapy based on Andro in NSCLC; (II) it can be developed multiple treatment ways that combination with Andro; (III) based on the mechanism of Andro in treating NSCLC, it can be developed some metabolic marker for prognosis estimation after taking Andro in NSCLC patients.

However, there are some limitations about this work. For example, we just launched the study *in vitro*, but not *in vivo*. We just adopted only one cell line due to the limited fees. Some lncRNA or miRNA may regulate the Andro, here, we just explored the role of Andro on NSCLC cell proliferation and apoptosis and explored whether its corresponding mechanism involved in mitochondrial apoptosis pathway and glucose metabolism pathway. These limitations will be supplemented in our following further experiments.

In summary, we showed that Andro inhibits the cell proliferation of NSCLC by activating the mitochondrial apoptosis pathway, restraining glycolysis, and promoting the gluconeogenesis pathway.

Acknowledgments

We would like to thank all the reviewers for their valuable comments and MJEditor (www.mjeditor.com) for their linguistic assistance during the preparation of this manuscript.
Funding: This research was supported by the Zhejiang Provincial Natural Science Foundation of China (Grant No. LQ19H280007).

Footnote

Reporting Checklist: The authors have completed the MDAR reporting checklist. Available at https://dx.doi.org/10.21037/atm-21-5975

Data Sharing Statement: Available at https://dx.doi.

org/10.21037/atm-21-5975

Conflicts of Interest: All authors have completed the ICMJE uniform disclosure form (available at https://dx.doi.org/10.21037/atm-21-5975). The authors have no conflicts of interest to declare.

Ethical Statement: The authors are accountable for all aspects of the work in ensuring that questions related to the accuracy or integrity of any part of the work are appropriately investigated and resolved.

References

1. Bade BC, Dela Cruz CS. Lung Cancer 2020: Epidemiology, Etiology, and Prevention. Clin Chest Med 2020;41:1-24.
2. Broderick SR. Adjuvant and Neoadjuvant Immunotherapy in Non-small Cell Lung Cancer. Thorac Surg Clin 2020;30:215-20.
3. Chen W, Zheng R, Baade PD, et al. Cancer statistics in China, 2015. CA Cancer J Clin 2016;66:115-32.
4. Reck M, Heigener DF, Mok T, et al. Management of non-small-cell lung cancer: recent developments. Lancet 2013;382:709-19.
5. Rotow J, Bivona TG. Understanding and targeting resistance mechanisms in NSCLC. Nat Rev Cancer 2017;17:637-58.
6. Lee JC, Tseng CK, Young KC, et al. Andrographolide exerts anti-hepatitis C virus activity by up-regulating haeme oxygenase-1 via the p38 MAPK/Nrf2 pathway in human hepatoma cells. Br J Pharmacol 2014;171:237-52.
7. Lin HH, Tsai CW, Chou FP, et al. Andrographolide down-regulates hypoxia-inducible factor-1α in human non-small cell lung cancer A549 cells. Toxicol Appl Pharmacol 2011;250:336-45.
8. Kuttan G, Pratheeshkumar P, Manu KA, et al. Inhibition of tumor progression by naturally occurring terpenoids. Pharm Biol 2011;49:995-1007.
9. Qi CL, Wang LJ, Zhou XL. Advances in study on anti-tumor mechanism of andrographolide. Zhongguo Zhong Yao Za Zhi 2007;32:2095-7.
10. Luo X, Luo W, Lin C, et al. Andrographolide inhibits proliferation of human lung cancer cells and the related mechanisms. Int J Clin Exp Med 2014;7:4220-5.
11. Yuwen D, Mi S, Ma Y, et al. Andrographolide enhances cisplatin-mediated anticancer effects in lung cancer cells through blockade of autophagy. Anticancer Drugs 2017;28:967-76.
12. Lee YC, Lin HH, Hsu CH, et al. Inhibitory effects of andrographolide on migration and invasion in human non-small cell lung cancer A549 cells via down-regulation of PI3K/Akt signaling pathway. Eur J Pharmacol 2010;632:23-32.
13. Terzioglu M, Larsson NG. Mitochondrial dysfunction in mammalian ageing. Novartis Found Symp 2007;287:197-208; discussion 208-13.
14. Kakkar P, Singh BK. Mitochondria: a hub of redox activities and cellular distress control. Mol Cell Biochem 2007;305:235-53.
15. Green DR, Kroemer G. The pathophysiology of mitochondrial cell death. Science 2004;305:626-9.
16. Tocchi A, Quarles EK, Basisty N, et al. Mitochondrial dysfunction in cardiac aging. Biochim Biophys Acta 2015;1847:1424-33.
17. Wang CH, Tsai TF, Wei YH. Role of mitochondrial dysfunction and dysregulation of Ca(2+) homeostasis in insulin insensitivity of mammalian cells. Ann N Y Acad Sci 2015;1350:66-76.
18. Gao J, Qiu X, Xi G, et al. Downregulation of GSDMD attenuates tumor proliferation via the intrinsic mitochondrial apoptotic pathway and inhibition of EGFR/Akt signaling and predicts a good prognosis in non-small cell lung cancer. Oncol Rep 2018;40:1971-84.
19. Liu WB, Xie F, Sun HQ, et al. Anti-tumor effect of polysaccharide from Hirsutella sinensis on human non-small cell lung cancer and nude mice through intrinsic mitochondrial pathway. Int J Biol Macromol 2017;99:258-64.
20. Chen CJ, Shih YL, Yeh MY, et al. Ursolic Acid Induces Apoptotic Cell Death Through AIF and Endo G Release Through a Mitochondria-dependent Pathway in NCI-H292 Human Lung Cancer Cells In Vitro. In Vivo 2019;33:383-91.
21. Dey SK, Bose D, Hazra A, et al. Cytotoxic activity and apoptosis-inducing potential of di-spiropyrrolidino and di-spiropyrrolizidino oxindole andrographolide derivatives.

PLoS One 2013;8:e58055.
22. Ferrarini A, Di Poto C, He S, et al. Metabolomic Analysis of Liver Tissues for Characterization of Hepatocellular Carcinoma. J Proteome Res 2019;18:3067-76.
23. Malakar P, Stein I, Saragovi A, et al. Long Noncoding RNA MALAT1 Regulates Cancer Glucose Metabolism by Enhancing mTOR-Mediated Translation of TCF7L2. Cancer Res 2019;79:2480-93.
24. Pavlides S, Whitaker-Menezes D, Castello-Cros R, et al. The reverse Warburg effect: aerobic glycolysis in cancer associated fibroblasts and the tumor stroma. Cell Cycle 2009;8:3984-4001.
25. Hanahan D, Coussens LM. Accessories to the crime: functions of cells recruited to the tumor microenvironment. Cancer Cell 2012;21:309-22.
26. Ma J, Qi G, Li L. A Novel Serum Exosomes-Based Biomarker hsa_circ_0002130 Facilitates Osimertinib-Resistance in Non-Small Cell Lung Cancer by Sponging miR-498. Onco Targets Ther 2020;13:5293-307.
27. Ji X, Qian J, Rahman SMJ, et al. xCT (SLC7A11)-mediated metabolic reprogramming promotes non-small cell lung cancer progression. Oncogene 2018;37:5007-19.
28. Lai YH, Yu SL, Chen HY, et al. The HLJ1-targeting drug screening identified Chinese herb andrographolide that can suppress tumour growth and invasion in non-small-cell lung cancer. Carcinogenesis 2013;34:1069-80.
29. Mi S, Xiang G, Yuwen D, et al. Inhibition of autophagy by andrographolide resensitizes cisplatin-resistant non-small cell lung carcinoma cells via activation of the Akt/mTOR pathway. Toxicol Appl Pharmacol 2016;310:78-86.
30. Qiu X, Shi L, Zhuang H, et al. Cerebrovascular Protective Effect of Boldine Against Neural Apoptosis via Inhibition of Mitochondrial Bax Translocation and Cytochrome C Release. Med Sci Monit 2017;23:4109-16.
31. Yang C, Zhu S, Yang H, et al. FBP1 binds to the bromodomain of BRD4 to inhibit pancreatic cancer progression. Am J Cancer Res 2020;10:523-35.
32. Zhang CC, Li CG, Wang YF, et al. Chemotherapeutic paclitaxel and cisplatin differentially induce pyroptosis in A549 lung cancer cells via caspase-3/GSDME activation. Apoptosis 2019;24:312-25.
33. Lu W, Zhang H, Niu Y, et al. Long non-coding RNA linc00673 regulated non-small cell lung cancer proliferation, migration, invasion and epithelial mesenchymal transition by sponging miR-150-5p. Mol Cancer 2017;16:118.
34. Yang B, Zhang L, Cao Y, et al. Overexpression of lncRNA IGFBP4-1 reprograms energy metabolism to promote lung cancer progression. Mol Cancer 2017;16:154.
35. Li R, Wang X, Zhang X, et al. Ad5-EMC6 mediates antitumor activity in gastric cancer cells through the mitochondrial apoptosis pathway. Biochem Biophys Res Commun 2019;513:663-8.
36. Sun WL, Wang L, Luo J, et al. Ambra1 inhibits paclitaxel-induced apoptosis in breast cancer cells by modulating the Bim/mitochondrial pathway. Neoplasma 2019;66:377-85.
37. Acuña UM, Mo S, Zi J, et al. Hapalindole H Induces Apoptosis as an Inhibitor of NF-κB and Affects the Intrinsic Mitochondrial Pathway in PC-3 Androgen-insensitive Prostate Cancer Cells. Anticancer Res 2018;38:3299-307.
38. Vaupel P, Schmidberger H, Mayer A. The Warburg effect: essential part of metabolic reprogramming and central contributor to cancer progression. Int J Radiat Biol 2019;95:912-9.
39. Hay N. Reprogramming glucose metabolism in cancer: can it be exploited for cancer therapy? Nat Rev Cancer 2016;16:635-49.
40. Zhang J, Lai Z, Huang W, et al. Apicidin Inhibited Proliferation and Invasion and Induced Apoptosis via Mitochondrial Pathway in Non-small Cell Lung Cancer GLC-82 Cells. Anticancer Agents Med Chem 2017;17:1374-82.
41. Zhai S, Zhao L, Lin T, et al. Downregulation of miR-33b promotes non-small cell lung cancer cell growth through reprogramming glucose metabolism miR-33b regulates non-small cell lung cancer cell growth. J Cell Biochem 2019;120:6651-60.
42. Yuan H, Sun B, Gao F, et al. Synergistic anticancer effects of andrographolide and paclitaxel against A549 NSCLC cells. Pharm Biol 2016;54:2629-35.
43. Yang S, Evens AM, Prachand S, et al. Mitochondrial-mediated apoptosis in lymphoma cells by the diterpenoid lactone andrographolide, the active component of Andrographis paniculata. Clin Cancer Res 2010;16:4755-68.
44. Yang L, Wu D, Luo K, et al. Andrographolide enhances 5-fluorouracil-induced apoptosis via caspase-8-dependent mitochondrial pathway involving p53 participation in hepatocellular carcinoma (SMMC-7721) cells. Cancer Lett 2009;276:180-8.
45. Mandal M, Adam L, Kumar R. Redistribution of activated caspase-3 to the nucleus during butyric acid-induced apoptosis. Biochem Biophys Res Commun 1999;260:775-80.
46. Gupta S, Knowlton AA. HSP60, Bax, apoptosis and the heart. J Cell Mol Med 2005;9:51-8.
47. Hu H, Jiang C, Schuster T, et al. Inorganic selenium sensitizes prostate cancer cells to TRAIL-induced apoptosis

through superoxide/p53/Bax-mediated activation of mitochondrial pathway. Mol Cancer Ther 2006;5:1873-82.
48. Hanahan D, Weinberg RA. Hallmarks of cancer: the next generation. Cell 2011;144:646-74.
49. Compan V, Pierredon S, Vanderperre B, et al. Monitoring Mitochondrial Pyruvate Carrier Activity in Real Time Using a BRET-Based Biosensor: Investigation of the Warburg Effect. Mol Cell 2015;59:491-501.
50. Zhong X, Tian S, Zhang X, et al. CUE domain-containing protein 2 promotes the Warburg effect and tumorigenesis. EMBO Rep 2017;18:809-25.
51. Hirata H, Sugimachi K, Komatsu H, et al. Decreased Expression of Fructose-1,6-bisphosphatase Associates with Glucose Metabolism and Tumor Progression in Hepatocellular Carcinoma. Cancer Res 2016;76:3265-76.
52. Yang J, Wang C, Zhao F, et al. Loss of FBP1 facilitates aggressive features of hepatocellular carcinoma cells through the Warburg effect. Carcinogenesis 2017;38:134-43.
53. Ma R, Zhang W, Tang K, et al. Switch of glycolysis to gluconeogenesis by dexamethasone for treatment of hepatocarcinoma. Nat Commun 2013;4:2508.
54. Feng J, Dai W, Mao Y, et al. Simvastatin re-sensitizes hepatocellular carcinoma cells to sorafenib by inhibiting HIF-1α/PPAR-γ/PKM2-mediated glycolysis. J Exp Clin Cancer Res 2020;39:24.
55. Shi J, Zhang Y, Qin B, et al. Long non-coding RNA LINC00174 promotes glycolysis and tumor progression by regulating miR-152-3p/SLC2A1 axis in glioma. J Exp Clin Cancer Res 2019;38:395.
56. Sai KKS, Zachar Z, Bingham PM, et al. Metabolic PET Imaging in Oncology. AJR Am J Roentgenol 2017;209:270-6.
57. Postmus PE, Kerr KM, Oudkerk M, et al. Early and locally advanced non-small-cell lung cancer (NSCLC): ESMO Clinical Practice Guidelines for diagnosis, treatment and follow-up. Ann Oncol 2017;28:iv1-iv21.
58. You X, Jiang W, Lu W, et al. Metabolic reprogramming and redox adaptation in sorafenib-resistant leukemia cells: detected by untargeted metabolomics and stable isotope tracing analysis. Cancer Commun (Lond) 2019;39:17.
59. Ying H, Kimmelman AC, Lyssiotis CA, et al. Oncogenic Kras maintains pancreatic tumors through regulation of anabolic glucose metabolism. Cell 2012;149:656-70.
60. Fong MY, Zhou W, Liu L, et al. Breast-cancer-secreted miR-122 reprograms glucose metabolism in premetastatic niche to promote metastasis. Nat Cell Biol 2015;17:183-94.
61. Ooi AT, Gomperts BN. Molecular Pathways: Targeting Cellular Energy Metabolism in Cancer via Inhibition of SLC2A1 and LDHA. Clin Cancer Res 2015;21:2440-4.
62. Menendez JA, Alarcón T. Metabostemness: a new cancer hallmark. Front Oncol 2014;4:262.
63. Rossello X, Yellon DM. The RISK pathway and beyond. Basic Res Cardiol 2018;113:2.
64. Shi HS, Li D, Zhang J, et al. Silencing of pkm2 increases the efficacy of docetaxel in human lung cancer xenografts in mice. Cancer Sci 2010;101:1447-53.
65. Cong J, Wang X, Zheng X, et al. Dysfunction of Natural Killer Cells by FBP1-Induced Inhibition of Glycolysis during Lung Cancer Progression. Cell Metab 2018;28:243-255.e5.
66. Beddow SA, Gattu AK, Vatner DF, et al. PEPCK1 Antisense Oligonucleotide Prevents Adiposity and Impairs Hepatic Glycogen Synthesis in High-Fat Male Fed Rats. Endocrinology 2019;160:205-19.
67. Bian XL, Chen HZ, Yang PB, et al. Nur77 suppresses hepatocellular carcinoma via switching glucose metabolism toward gluconeogenesis through attenuating phosphoenolpyruvate carboxykinase sumoylation. Nat Commun 2017;8:14420.
68. Zhou H, Yue Y, Wang J, et al. Melatonin therapy for diabetic cardiomyopathy: A mechanism involving Syk-mitochondrial complex I-SERCA pathway. Cell Signal 2018;47:88-100.
69. Vaz CV, Marques R, Alves MG, et al. Androgens enhance the glycolytic metabolism and lactate export in prostate cancer cells by modulating the expression of GLUT1, GLUT3, PFK, LDH and MCT4 genes. J Cancer Res Clin Oncol 2016;142:5-16.
70. Huo X, Wang C, Yu Z, et al. Human transporters, PEPT1/2, facilitate melatonin transportation into mitochondria of cancer cells: An implication of the therapeutic potential. J Pineal Res 2017. doi: 10.1111/jpi.12390.
71. Xu RH, Pelicano H, Zhou Y, et al. Inhibition of glycolysis in cancer cells: a novel strategy to overcome drug resistance associated with mitochondrial respiratory defect and hypoxia. Cancer Res 2005;65:613-21.

(English Language Editor: A. Kassem)

Cite this article as: Chen Z, Tang WJ, Zhou YH, Chen ZM, Liu K. Andrographolide inhibits non-small cell lung cancer cell proliferation through the activation of the mitochondrial apoptosis pathway and by reprogramming host glucose metabolism. Ann Transl Med 2021;9(22):1701. doi: 10.21037/atm-21-5975